Life-Cycle of Structures and Infrastructure Systems – Biondini & Frangopol (Eds)

The hydration of cement paste: Thermodynamics driven multi-scale modeling of elastic properties and coda wave interferometry based monitoring

E. Jägle, J.J. Timothy, F. Diewald, T. Kränkel & C. Gehlen
Chair of Materials Science and Testing, Department of Materials Engineering, TUM School of Engineering and Design, Centre for Building Materials, Technical University of Munich, Munich, Bavaria, Germany

A. Machner
Professorship for Mineral Construction Materials, Department of Materials Engineering, TUM School of Engineering and Design, Centre for Building Materials, Technical University of Munich, Munich, Bavaria, Germany

ABSTRACT: Concrete is produced by mixing hydraulic cement and aggregates with water. In contact with water, the cement particles first dissolve and subsequently hydrates form through various chemical reactions determining the overall mechanical material properties. Modeling, simulation, and monitoring of the cement hydration provide insights into the processes involved and allow prediction of overall material properties. Thereby, linking the underlying chemical processes to macroscopic material properties remains a key challenge. In this contribution, thermodynamic simulation and a multi-scale modeling approach were employed for Young's modulus development prediction for an ordinary Portland cement paste during the first 24°h of hydration. Further, ultrasound based Coda Wave Interferometry (CWI) methods were applied for monitoring of corresponding cement paste specimens. Coinciding trends were found for model and monitoring based results: Initial small alterations are followed by a period of strong material changes with an accelerated stiffness development and a strong increase in wave velocity.

1 INTRODUCTION

Reinforced concrete is used extensively for the construction of infrastructure around the globe. To produce concrete, cement, and aggregates are mixed with water. Through various reactions of the cement with the water, a cement paste matrix is formed, binding the aggregates together and leading to the overall solidification and strength development of the material. This process is referred to as hydration. The hydration determines the short- and long-term strength of concrete and is therefore an essential part of holistic durability assessment. Previous researchers have focused on understanding and predicting the chemical processes (e.g., Ouzia & Scrivener 2019; Lothenbach & Zajac 2019), strength and stiffness development (e.g., Pichler et al. 2009), as well as the development of new monitoring methods (e.g., Diewald et al. 2022b). Nevertheless, it remains challenging to link the complex microstructural changes to macroscopic material properties. Advances have been made in thermodynamic simulation of the chemical reactions, including the development of a web application (CemGEMS) for thermodynamic simulations by Kulik et al. (2021). Using existing concepts of multi-scale modeling for macroscopic material properties there is potential to predict stiffness development during hydration based on thermodynamic simulation results. Such predictions need to be validated by experimental information. Therefore, in-situ monitoring of material changes is required. Recently, ultrasound (US) based Coda Wave Interferometry (CWI) is extensively

DOI: 10.1201/9781003323020-226

investigated for low-cost, in-situ monitoring of concrete structures (Diewald et al. 2022a). Diewald et al. (2022b) applied CWI methods for investigating early hydration and compared the respective results to conventional hydration monitoring techniques.

2 THEORETICAL BACKGROUND

2.1 *Microstructure development during cement hydration*

Cement is a multi-phase material, which is comprised of the cement clinker, calcium sulfates such as gypsum and anhydrite, and optional mineral additives. In ordinary Portland cement (OPC), the cement clinker is the main component (Taylor 1997). Within the clinker, grains of alite (C_3S) and belite (C_2S) are bound together by aluminate (C_3A) and ferrite (C_4AF) (Stutzman 2004). When the cement is mixed with water, it dissolves and hydrates form out of the aqueous solution, which build the solid cement paste matrix. The main hydrates during early hydration up to 24 h are needle shaped calcium silicate hydrates (C-S-H), plate-like portlandite (CH), and ettringite needles (AFt) (Scrivener 1984). Other phases might occur in smaller quantities (Scrivener 1984; Li et al. 2022), including plates of monocarbonate, flake-like hydrotalcite, or spherical hydrogarnet. The hydrates precipitate mainly on or near the cement grain surface and grow, leading to the connection of individual cement grains, when a certain hydration degree (percolation threshold) is reached (Garboczi & Bentz 1998; Torrenti & Benboudjema 2005). The development of the microstructure through hydrate formation and percolation causes the transition of the initial workable, liquid mixture to a solid material. The related development of elastic properties, such as the Young's modulus is therefore intrinsically linked to the underlying chemical reactions.

2.2 *Thermodynamic simulation*

Thermodynamic modeling and simulation provide information on the thermodynamically stable phase assemblage at a certain degree of reaction of the cement and therefore indicate microstructural changes. It predicts hydrate formation based on cement consumption and thermodynamic information. Appropriate thermodynamic data for cement based systems is available through databases (Lothenbach et al. 2019). For predictions, the hydration process is typically depicted in two steps (Lothenbach & Zajac 2019): (I) Modeling of cement dissolution. (II) Thermodynamic simulation of hydrate formation. Forecasts on cement dissolution are usually based on empirically derived models, e.g., by Parrott & Killoh (1984). As their model was developed using long-term data, it has been reported by Kulik et al. (2021) to insufficiently describe cement dissolution during early hydration. Alternatively, they propose to use the five-parameter logistic (5PL) function fitted to experimentally obtained dissolution data. Given the dissolution information, thermodynamic calculations predict the phase assemblage as the most stable composition at the temperature and pressure stated, while simultaneously considering all aqueous, solid, and gaseous phases. Therefore, thermodynamic equilibrium is assumed, i.e., that the system has reached its most stable state under the given external conditions. However, during hydration, the system changes extensively, especially within the first hours. Thus, the equilibrium condition is not met during early hydration and calculations need to be restrained to mirror experimental observations. Therefore, the formation of certain phases is suppressed, as their formation is kinetically hindered.

Common software solutions for thermodynamic calculation, such as GEMS (Kulik et al. 2012), use the Gibbs free energy minimization approach to predict hydrate formation. Methods and software are under continuous improvement. Recently Kulik et al. (2021) developed the web application CemGEMS based on the GEMS-Selektor code and thermodynamic information from established databases for facilitated thermodynamic simulations. Customizable templates enable individual adjustments for the cement paste mixture and hydration conditions. They further provide simulation options including dissolution modeling according to the 5PL function.

2.3 *Microstructure modeling*

As discussed above, the microstructure of hydrating cement is heterogeneous. The properties of such a heterogeneous material can be described using the concept of a representative elementary volume (REV). An REV describes a volume (length scale L) containing heterogeneities (length scale l). The size of the REV is chosen such that $l \ll L$. The REV represents the effective behavior of a heterogeneous structure. If the properties of the individual constituents in the REV are given, the corresponding overall property can be obtained by homogenization using analytical or computational methods. If multiple geometries over a wide range of scales are involved, REVs are specified at each scale and homogenization is performed sequentially. In general, the stiffness (henceforth, the fourth order tensor of elasticity will be called the stiffness) of an REV with n different components with n different stiffness can be estimated using the following expression (Timothy & Meschke 2016):

$$\mathbb{C}_{REV} = \sum_{i=1}^{n} \phi_i \mathbb{C}_i : \mathbb{A}_i \tag{1}$$

In the above equation, $\mathbb{C}_{REV}$ is the homogenized and effective stiffness of the REV; $\mathbb{C}_i$ is the stiffness and ϕ_i the volume fraction of the i^{th} component. The fourth order tensor $\mathbb{A}_i$ is the localization tensor that downscales an applied strain at the REV level to the phase level. It also specifies geometrical information corresponding to the i^{th} material component. The localization tensor can be approximated by several methods depending on the material morphology (i.e. spatial distribution of the phases in an REV). For a material with a clear matrix-inclusion morphology, the Mori-Tanaka (MT) method can be used (Timothy & Meschke 2016):

$$\mathbb{C}_{REV}^{MT} = \mathbb{C}_h + \sum_{i=1}^{n} \phi_i (\mathbb{C}_i - \mathbb{C}_h) : \mathbb{A}_i : \left[\phi_h \mathbb{I} + \sum_{i=1}^{n} \phi_i \mathbb{A}_i \right]^{-1} \tag{2}$$

$$\mathbb{A}_i = \left[\mathbb{I} + \mathbb{S} : \mathbb{C}_h^{-1} : (\mathbb{C}_i - \mathbb{C}_h) \right]^{-1} \tag{3}$$

In the above expression, $\mathbb{S}$ is the Eshelby tensor and $\mathbb{C}_h$ is the elastic tensor of the matrix (host) phase. In case there is no clear matrix-inclusion morphology, but the phases are mixed together, the cascade micromechanics model (CCM) can be applied.

$$\mathbb{C}_{REV}^{CCM}(n+1) = \sum_{i=1}^{n} \phi_i \mathbb{C}_i : \mathbb{A}_i(n) : \left[\sum_{i=1}^{n} \phi_i \mathbb{A}_i(n) \right]^{-1} \tag{4}$$

$$\mathbb{A}_i(n) = \left[\mathbb{I} + \mathbb{S} : \mathbb{C}_{REV}^{-1}(n) : \left(\mathbb{C}_i - \mathbb{C}_{REV}^{-1} \right) \right]^{-1} \tag{5}$$

At $n \to \infty$ the self-consistent scheme is recovered. In this paper the Mori-Tanaka scheme and the CCM model (Timothy & Meschke 2016) at the regularized self-consistent limit is used.

2.4 *Ultrasound based monitoring with CWI methods*

State-of-the-art transmission techniques for US based hydration monitoring assess the development of wave velocity. A concise overview of these methods is given by Gabrijel et al. (2020). Currently, a new US approach is under investigation for monitoring reinforced concrete structures: Coda Wave Interferometry (CWI) uses multiply scattered waves for the detection of even marginal material changes. The term coda thereby refers to the tail of the US signal (Aki 1985), which contains information from these waves. Multiply scattered waves sample the material extensively, and therefore the coda is more sensitive to material changes than the direct wave.

Numerically, two waves recorded at different times $u(t')$ and $\tilde{u}(t')$ can be compared by a time-shifted correlation coefficient with a center-time t, and a window length from t_1 to t_2 (Snieder 2006). The stretching technique (Lobkis & Weaver 2003) describes the change in the waveform via stretching or compression such that the correlation coefficient $CC(\varepsilon)$ is maximized:

$$CC(\varepsilon) = \frac{\int_{t_1}^{t_2} u(t')\tilde{u}(t'(1-\varepsilon))\,\mathrm{d}t'}{\sqrt{\int_{t_1}^{t_2} u^2(t')\,\mathrm{d}t \int_{t_1}^{t_2} \tilde{u}^2(t'(1-\varepsilon))\,\mathrm{d}t'}} \tag{6}$$

The stretching factor ε thereby corresponds to the velocity variation $\mathrm{d}v/v$:

$$\varepsilon = \frac{\mathrm{d}v}{v} \tag{7}$$

Signals can be compared stepwise, or relative to a fixed reference signal. When using a stepwise reference, the cumulated velocity variation ε_c for the nth signal can be calculated as well:

$$\varepsilon_c = \begin{cases} \varepsilon_n, & n = 1 \\ (\varepsilon_{n-1} + 1)(\varepsilon_n + 1) - 1, & n > 1 \end{cases} \tag{8}$$

CWI is usually applied for the detection of subtle material alterations. Cement hydration, however, is associated with major changes in the material structure and properties. Nevertheless, the application of CWI methods with stepwise comparison enables tracing of time-dependent modifications. The ability of stepwise CWI to capture trends during early hydration was shown by Diewald et al. (2022b) by comparing CWI results for repeated US measurements for OPC concrete to corresponding information from conventional monitoring and thermodynamic simulation.

3 METHODS

3.1 *Thermodynamic simulation*

CemGEMS (Kulik et al. 2021) was used for the thermodynamic simulation of the cement phase assemblage during the first 24 h of hydration. Therefore, the phase assemblage of the anhydrous cement used for the US experiments as determined by quantitative X-ray diffraction, the water-to-cement ratio of 0.45, and conditions of 20 °C and 1 bar were implemented. For hydration simulation, the 5PL dissolution modeling approach was selected, setting the process parameters as proposed by CemGEMS. The calculation was performed for 24 h with 101 linear steps. To prohibit the formation of corresponding, kinetically hindered phases, the formation of specified phases, e.g., gibbsite and dolomite, were disabled as proposed by CemGEMS, and phosphorus, titanium, and manganese containing oxides were removed from the cement composition.

3.2 *Multi-scale modeling*

In order to model the evolution of the elastic properties of hydrating cement paste, a multi-level micromechanics homogenization model that uses the Mori-Tanaka and the CCM model was employed. The temporal evolution of the volume content of the material phases was obtained from the CemGEMS thermodynamic simulation. The corresponding elastic properties were obtained from literature (Haecker et al. 2005). To use Equation 1 and 2 also the geometry of the phases had to be specified. The hydrate phases C-S-H and ettringite are assumed to be needle-shaped (prolate spheroidal) while portlandite and monocarbonate are assumed to be disc shaped (oblate spheroidal). All other phases are assumed to be spherical in shape. All phases are assumed to be isotropically distributed. In total 6 REVs are used to upscale the elastic properties of hydrating cement paste. The REVs used in the homogenization procedure are shown in Figure 1.

REV-1 is modeled as a mixture of aluminate and ferrite without a clear matrix-inclusion morphology. Here the CCM model is applied. REV-2 corresponds to alite and belite embedded in a material mixture whose properties are obtained by homogenization of REV-1. The Mori-Tanaka scheme is applied for the homogenization of REV-2. REV-3 represents a heterogeneous

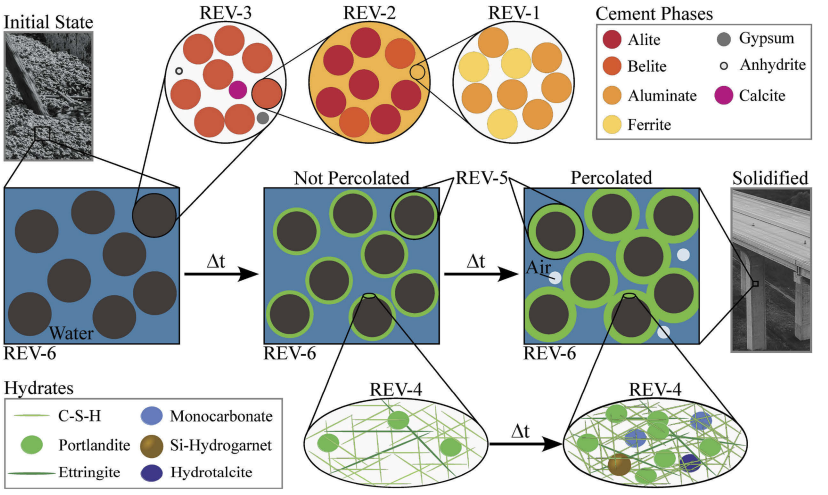

Figure 1. Schematic representation of the multi-scale model for stiffness development based on thermodynamically predicted phase assemblage by volume. All geometries represent 3-dimensional objects. For the representative elementary volumes REV-1 to REV-5 the material properties are homogenized and used as input for the larger scale REV. Through homogenization of REV-6 the overall material stiffness is obtained.

mixture of particles such as gypsum, anhydrite, calcite and the material phase whose properties have been obtained from homogenization of REV-2. As no clear matrix-inclusion morphology can be specified, the CCM model is used for homogenization of REV-3. The cement phase, i.e., REV-3 surrounded by REV-4 that represents the hydrates, is homogenized using the Mori-Tanaka scheme. This morphology refers to REV-5. REV-5 is finally embedded in the aqueous solution. REV-5 together with the aqueous solution is homogenized using the CCM model to obtain the effective elastic properties of REV-6. The evolution of the elastic properties using multi-scale homogenization was simulated using PyMatSim a Python based research software for materials simulation currently developed by the authors.

3.3 *Ultrasound based monitoring with CWI methods*

Cement paste with a water-to-cement ratio of 0.45 was produced using a CEM I 42.5 R with a density of 3.12 g/cm^3 and a Blaine specific surface of 3,400 cm^2/g. The raw materials were equilibrated at 20 °C and 37.619 kg of CEM I 42.5 R and 16.928 kg of tap water were mixed using a compulsatory mixer with a capacity of 75 L for a total of 150 s. Each specimen was prepared with two piezoelectrical US transducers symmetrically embedded at a distance of 300 mm. Figure 2 shows (A) one US transducer (ACSYS S0807) with a center frequency of 60 kHz, (B) the transducer positioning within the specimen, and (C) one specimen with embedded transducers after solidification and demolding. After casting, the specimens were covered with a moist jute cloth and stored in a climate chamber at 20 °C and 65 % relative humidity.

The US transducers were connected to the measuring system, which transmits pulses with a frequency of 60 kHz to the selected transducer and records the signal at the corresponding

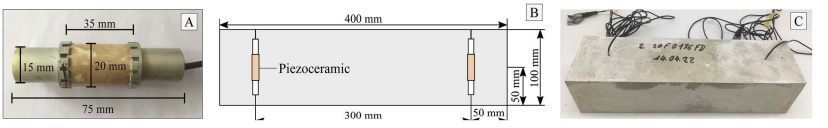

Figure 2. (A) New piezoelectrical US transducer. (B) Symmetrical transducer positioning within 400x100x100 mm^3 specimen for US monitoring. (C) Solidified CEM I 42.5 R pure cement paste specimen after demolding with two embedded US transducers as illustrated in (B). The mean temperature of the sample during the first 24 h of hydration was determined as approximately 30 °C.

receiver with a sampling rate of 2 MHz and 10,000 samples. Signals were collected every 5 min for the first 22 h with both embedded transducers acting as a sender and receiver once.

The recorded signals were processed by performing offset compensation, pretrigger, and crosstalk removal as well as frequency filtering as described by Niederleithinger et al. (2018). Further, the signals were clipped to the length of 4,500 μs and faulty signals were removed for which the maximum amplitude was less than 0.1 times the amplitude of the previous signal or with a maximum tail amplitude exceeding half the maximum amplitude of the early signal and maximum amplitudes greater than the noise.

4 RESULTS AND DISCUSSION

The simulated cement phase assemblage for the first 24 h of cement hydration in terms of volume fractions is shown in Figure 3(A). The thermodynamic simulation predicts a continuous decline in clinker content and an increase in hydrate volumes with increasing hydration time. Thereby, the total volume loss of solid and liquid phases was compensated artificially by the addition of air. The volume loss appears as a linear trend over time. However, the alterations of phase assemblage of cement phases and hydrates follow a non-linear behavior with striking events occurring between 6 h and 9 h: After about 7 h of hydration, gypsum disappears and at about 8 h the slope of volume increase in solid phases decreases. Moreover, from 8 h onwards, less ettringite is formed. The associated evolution of the material structure, expressed using the Young's modulus predicted by the multi-scale model is shown in Figure 3(B). Within the first hours, the Young's modulus increases only marginally below 0.1 GPa until the increase becomes visible at approximately 5 h of hydration and further accelerates after about 6 h. From this point on, the Young's modulus increases monotonously. After 24 h a maximum value of 8.65 GPa is reached.

The results of the CWI-based monitoring are shown in Figure 3(C)-(E). The entire processed signals were used to calculate the velocity variation dv/v, the correlation coefficient CC and the cumulated velocity variation ε_c by stepwise comparison according to Equations 6-8. The general trends are consistent with those reported by Diewald et al. (2022b). Initially, a 4 h long period of stagnating values is observed for all CWI parameter. Subsequently, strong changes occur between 4 h and 12 h, and a transition to minor parameter changes takes place from 12 h onwards. Within the first hours, the velocity variation fluctuates around zero due to noise dominating signal alterations. A switching process in the early signal leads to stabilization of the corresponding correlation coefficient within this period. During the second period, the velocity variation drops to negative values, indicating a velocity increase. Meanwhile, the correlation coefficient first deviates from and subsequently converges again to 1 as the US signals initially develop and later stabilize. Corresponding to the velocity variation, the cumulative velocity variation decreases to negative values within the second period and merges into a trend of smaller slope in the last hours.

The development of the cumulated velocity variation and the Young's modulus correlate, as both exhibit an initial period of no alteration, followed by a monotonous trend of declining or increasing values. This compliance can be explained by the underlying microstructure development: At first, the fluid suspension of solid particles in water does not yield significant stiffness. This remains unchanged until a certain hydration degree is reached, at which point the hydrates have grown so that the individual particles are bonded together. Progressing connectivity leads to the development of a continuous solid matrix and its densification. Consequently, the stiffness and the wave velocity increase, whereby the increase in velocity is reflected in an increasingly negative cumulated velocity variation. However, the transition time from the initial to the second phase differs between the model based prediction and experimental observations by about 2 h. This discrepancy is assumed to be mainly attributed to the difference in temperature, which is 20 °C for the model based results and 30 °C for the experimental data. The temperature has a major influence on the hydration progress and can enhance the hydration in the range of hours.

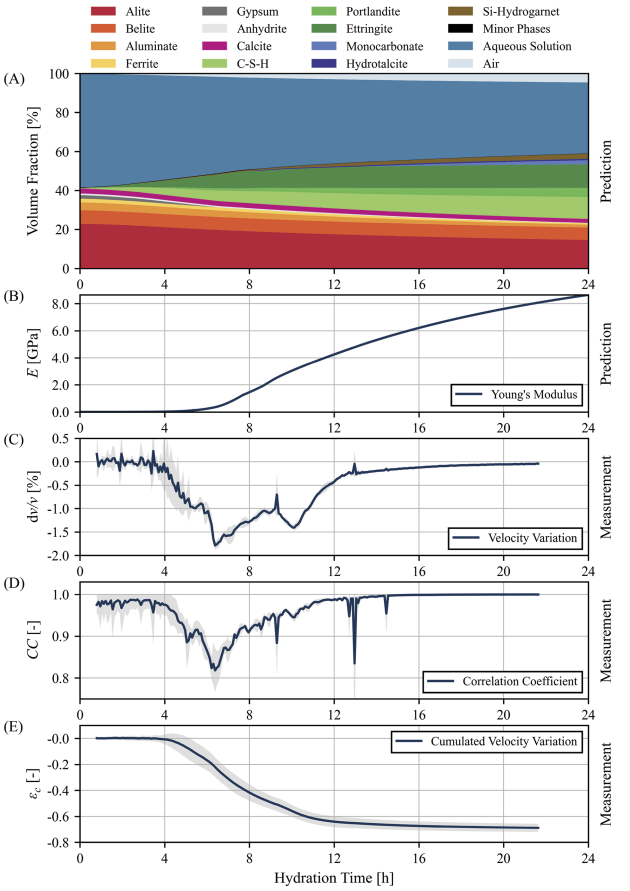

Figure 3. Thermodynamically predicted cement paste phase assemblage over hydration time at 20 °C (A). Composition as volume fractions relative to initial cement paste volume. Volume loss due to chemical shrinkage is compensated by air. (B) Young's modulus E, predicted by multi-scale modeling based on the thermodynamic prediction at 20 °C. Velocity variation dv/v (C), correlation coefficient CC (D), and cumulative velocity variation ε_c (E) retrieved by CWI with a stepwise comparison. Average values (solid blue lines) and standard deviation (grey shadowed areas) from two specimens and two measurement directions each. Specimens for US monitoring exhibited an average temperature of approximately 30 °C during the observed period.

5 CONCLUSIONS

In this study, thermodynamic simulation of cement paste phase assemblage was combined with a multi-scale model for stiffness prediction. The development of the Young's modulus retrieved was compared to experimental results of US monitoring using CWI methods. The validity of the model was indicated by correlation of the Young's modulus and the cumulated velocity variation. A period of major microstructural change was observed within the predicted phase assemblage, Young's modulus development, and the CWI parameter at about 4 to 8 hours of hydration. Agreement of results is limited by the thermodynamic equilibrium assumption and a hydration temperature of 20 °C, which underlie the thermodynamic simulation and the idealized stiffness model.

The feasibility and potential of an integrated approach, combining thermodynamic simulation, multi-scale modeling, and CWI monitoring was demonstrated. Further refinement of the models and simulations, as well as the evaluation by means of corresponding experimental data, is required for improved predictions. A deepened understanding of CWI parameter

development during hydration seems further promising for the linkage of microstructural developments to macroscopic material properties.

ACKNOWLEDGEMENTS

We thank the German Research Foundation (DFG) for the funding of the Research Unit FOR 2825 (project number 398216472). This research was enabled in the framework of Subprojects TUM1 and RUB1 with the provided measurement devices of BAM. We thank Sara Niedenzu, Felix Bachl, Manuel Gebhart and Karin Hartlieb-Pfüller for their valuable contribution.

REFERENCES

Aki, K. 1985. Theory of Earthquake Prediction with Special Reference to Monitoring of the Quality Factor of Lithosphere by the Coda Method. In C. Kisslinger & T. Rikitake (eds), *Practical Approaches to Earthquake Prediction and Warning*: 219–230. Dordrecht: Springer Netherlands.

Diewald, F. et al. 2022a. Impact of External Mechanical Loads on Coda Waves in Concrete. *Materials* 15 (16): 5482.

Diewald, F. et al. 2022b. Monitoring Early Cement Hydration with Coda Wave Interferometry. In S. Farhangdoust et al. (eds), *Proceedings of the 13th International Workshop on Structural Health Monitoring*: 141–148. Stanford.

Gabrijel, I. et al. 2020. Ultrasonic Techniques for Determination and Monitoring Various Properties of Cementitious Materials at Early Ages. In M. Serdar et al. (eds), *Advanced Techniques for Testing of Cement-Based Materials*: 23–68. Cham: Springer International Publishing.

Garboczi, E.J. & Bentz, D.P. 1998. The microstructure of portland cement-based materials: computer simulation and percolation theory. In *Proceedings of the Spring 1998 Materials Research Society on Computational Materials Science*: 89–100. San Francisco.

Haecker, C.-J. et al. 2005. Modeling the linear elastic properties of Portland cement paste. *Cement and Concrete Research* 35(10): 1948–1960.

Kulik, D.A. et al. 2012. GEM-Selektor geochemical modeling package: revised algorithm and GEMS3K numerical kernel for coupled simulation codes. *Computational Geosciences* 17: 1–24.

Kulik, D.A. et al. 2021. CemGEMS – an easy-to-use web application for thermodynamic modeling of cementitious materials. *RILEM Technical Letters* 6: 36–52.

Li, B. et al. 2022. The Early Age Hydration Products and Mechanical Properties of Cement Paste Containing GBFS under Steam Curing Condition. *Buildings* 12(10): 1746.

Lobkis, O.I. & Weaver, R.L. 2003. Coda-wave interferometry in finite solids: recovery of P-to-S conversion rates in an elastodynamic billiard. *Physical review letters* 90(25): 254302.

Lothenbach, B. et al. 2019. Cemdata18: A chemical thermodynamic database for hydrated Portland cements and alkali-activated materials. *Cement and Concrete Research* 115: 472–506.

Lothenbach, B. & Zajac, M. 2019. Application of thermodynamic modelling to hydrated cements. *Cement and Concrete Research* 123: 105779.

Niederleithinger, E. et al. 2018. Processing Ultrasonic Data by Coda Wave Interferometry to Monitor Load Tests of Concrete Beams. *Sensors* 18(6): 1971.

Ouzia, A. & Scrivener, K. 2019. The needle model: A new model for the main hydration peak of alite. *Cement and Concrete Research* 115: 339–360.

Parrott, L.J. & Killoh, D.C. 1984. Prediction of Cement Hydration. *British Ceramic Procedures* 35: 41–53.

Pichler, B. et al. 2009. Spherical and acicular representation of hydrates in a micromechanical model for cement paste: predic-tion of early-age elasticity and strength. *Acta Mechanica* 203(3): 137–162.

Scrivener, K. 1984. *The development of microstructure during the hydration of cement*. PhD Thesis: Imperial College.

Snieder, R. 2006. The Theory of Coda Wave Interferometry. *Pure and applied geophysics* 163: 455–473.

Stutzman, P. 2004. Scanning electron microscopy imaging of hydraulic cement microstructure. *Cement and Concrete Composites* 26(8): 957–966.

Taylor, H.F.W. 1997. *Cement Chemistry*. London: Thomas Telford Publishing.

Timothy, J.J. & Meschke, G. 2016. A cascade continuum micromechanics model for the effective elastic properties of porous materials. *International Journal of Solids and Structures*, 83: 1–12.

Torrenti, J.M. & Benboudjema, F. 2005. Mechanical threshold of cementitious materials at early age. *Materials and Structures* 38(3): 299–304.